

## Nonconventional methods for obtaining hexaferrites

### II. Barium hexaferrite

Oana Carp<sup>a,\*</sup>, Ruxandra Barjega<sup>b</sup>, E. Segal<sup>c</sup>, Maria Brezeanu<sup>d</sup>

<sup>a</sup> *Institute of Physical Chemistry, Splaiul Independentei, Nr. 202, Sector 6, Bucharest, Romania*

<sup>b</sup> *ZECASIN SA, Chemical Research & Development & Production, Splaiul Independentei, Nr. 202, Sector 6, Bucharest, Romania*

<sup>c</sup> *Department of Physical Chemistry, Faculty of Chemistry, University of Bucharest, Bd. Republicii 13, Bucharest, Romania*

<sup>d</sup> *Department of Inorganic Chemistry, University of Bucharest, Dumbrova Rosie Street, Nr. 23, Sector 2, Bucharest, Romania*

Received 13 September 1997; accepted 16 April 1998

#### Abstract

Small particles of barium hexaferrite ( $\text{BaFe}_{12}\text{O}_{19}$ ) were synthesized by thermal decomposition of precursors obtained by a new coprecipitation method. The influence of precursors' history upon their thermal behavior and phase composition evolution were investigated. © 1998 Elsevier Science B.V.

*Keywords:* Barium hexaferrite; Nonconventional methods; Precursors

#### 1. Introduction

Among the different classes of magnetic materials, hexagonal hard ferrites such as barium ferrite have attracted much attention because of their potential application in permanent magnets, microwave devices and magnetic recording media [1–3].

Fine particles of such ferrites cannot be produced easily and routinely by the conventional mixed oxide ceramic method (which involves the calcination of a mixture of  $\text{BaCO}_3$  and  $\alpha\text{-Fe}_2\text{O}_3$  at ca.  $1200^\circ\text{C}$ ). Under such conditions, wet chemical methods are nowadays used for achieving this goal. Correspondingly, we developed some precursor's methods – which consist in obtaining solid precursors of mixed oxides, in which the metallic ions present in a proper ratio are

already mixed at atomic scale. We reported in a previous work some results concerning the obtaining of lead hexaferrite [4].

This paper presents our results about the synthesis of fine barium hexaferrite, using as precursors some hydroxy-oxalate coprecipitates. Special emphasis is given on the influence of precursors' history upon their thermal behavior.

#### 2. Experimental

The mixed oxide's precursors were obtained by a chemical coprecipitation technique. So, dilute  $\text{NH}_4\text{OH}$  or  $\text{NaOH}$  solutions (25% w/w) were added to the suspensions of iron oxalate ( $\text{FeC}_2\text{O}_4 \cdot 2\text{H}_2\text{O}$ , reagent grade) and a barium salt ( $\text{Ba}(\text{CH}_3\text{COO})_2 \cdot 2\text{H}_2\text{O}$  or  $\text{Ba}(\text{NO}_3)_2$ , reagent grade). The copre-

\*Corresponding author.

precipitations were performed at  $\text{pH} \sim 12$ , and at room temperature. The coprecipitates were then filtered off and washed with water.

The composition of the precursors was determined by quantitative analysis: the metal content by gravimetric technique, and the carbon, hydrogen and nitrogen contents by using a combustion method coupled with chromatographic techniques.

In order to characterize the precursors as well as their calcination products, IR spectrometry, X-ray diffraction, thermal analysis and magnetic measurements were applied.

The IR spectra were recorded with a BIO-RAD FTIR 1255 spectrophotometer type.

The X-ray diffractograms were recorded with a DRON 3 X-ray diffractometer with  $\text{CoK}_\alpha$  radiation.

The heating curves (TG-DTG-DTA) were obtained by using Paulik–Paulik–Erdey type Q-1500 derivatograph, in static air, at various heating rates. Samples weighing 100 mg were used. In order to record the DTA curves,  $\alpha$ -alumina was used as inert material.

The magnetic properties (the saturation magnetization) at room temperature of the final decomposition products were determined by means of permeameter method.

### 3. Results and discussion

#### 3.1. Precursors

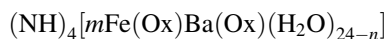
Although slight modification of the synthesis conditions lead to changes of the chemical composition of the synthesized precursors, the following general formulas may be written for the compounds obtained with the two precipitating agents:

- (a) for the case of the precipitation with NaOH



where  $m'+n=10.5; 11; 11.5; 12$  and  $0 < x < 12$ .

- (b) for the case of the precipitation with  $\text{NH}_4\text{OH}$  solution



where  $m=10.5; 11; 11.5; 12$  and  $0 < x < 12$ .

The IR spectra pointed out that all the four precursors are present in the structural skeleton of

$\text{FeC}_2\text{O}_4 \cdot 2\text{H}_2\text{O}$  The precursors obtained during the precipitation with NaOH solution contain a reduced amount of oxalate anions (approximately half). This statement is supported qualitatively by the decrease in intensities corresponding to the IR bands of oxalate anions and quantitatively by chemical elemental analysis. The remaining amount of iron is present as  $\gamma\text{-FeOOH}$  (IR analysis confirmed the identification), the synthesis conditions being favorable to a partial oxidation of the  $\text{Fe}^{2+}$  ions. Traces of  $\gamma\text{-FeOOH}$  were also identified in the first type of precursors. ( $\sim 3\text{--}5\%$ )

From the crystallinity point of view, the two types of precursors are very different. While amorphous solids are obtained by precipitation with NaOH, crystalline ones are obtained in the case of precipitation with  $\text{NH}_4\text{OH}$  solution. In the latter, the X-ray diffraction data pointed to the presence of a mixture consisting of two well-crystallized phases: monoclinic iron oxalate  $\text{FeC}_2\text{O}_4 \cdot 2\text{H}_2\text{O}$  (ASTM 23-293) and triclinic barium oxalate  $\text{BaC}_2\text{O}_4 \cdot 3\text{H}_2\text{O}$  (ASTM 23-67). A higher crystallinity was found for the precursors with  $\text{BaNO}_3$  as starting material. The crystalline phases are characterized by broad diffraction lines indicating small particles. The mean crystallite sizes, calculated by Sherer' [5] formula from the four most intense diffraction lines, vary in the 250–300 Å range.

#### 3.2. Nonisothermal and isothermal analyses of the precursors

As the investigated compounds represent precursors for mixed oxides, the goals of the nonisothermal and isothermal investigations are:

- to determine the temperature range of occurrence and the stoichiometry of the thermal transformations; and
- to establish how the history of compounds may influence their thermal behavior and quality of the final mixed oxide.

The investigated precursors undergo decompositions in several steps (5–6), the final decomposition temperatures for all studied compound being close to  $900^\circ\text{C}$ . No phase transformations were in evidence. Due to their comparable composition and structure, the thermal transformations of the precursors obtained during the precipitation with the same agent occur with similar stoichiometry in the same temperature

Table 1  
Thermal analysis of the investigated precursors

Precursor	$T_i - T_f$ <sup>a</sup> /°C	Mass loss/%	Thermal effect	Assignment
Ba(CH <sub>3</sub> COO) <sub>2</sub> -FeC <sub>2</sub> O <sub>4</sub> (NH <sub>4</sub> OH)	58–100	3.86	endo	humidity water release
	100–180	17.09	endo	NH <sub>4</sub> OH and lattice water release
	180–308	28.00	exo	decomposition of iron oxalate to $\gamma$ -Fe <sub>2</sub> O <sub>3</sub>
	408–510	1.04	exo	decomposition of barium oxalate to barium carbonate
	660–835	1.47	exo	reaction in solid state between iron oxide and barium carbonate, formation of barium hexaferrite
Total:	51.46			
Ba(NO <sub>3</sub> ) <sub>2</sub> -FeC <sub>2</sub> O <sub>4</sub> (NH <sub>4</sub> OH)	55–104	2.41	endo	humidity water release
	104–170	14.37	endo	NH <sub>4</sub> OH and lattice water release
	170–286	29.38	exo	decomposition of iron oxalate to $\gamma$ -Fe <sub>2</sub> O <sub>3</sub>
	407–502	1.18	exo	decomposition of barium oxalate to barium carbonate
	687–850	1.76	exo	reaction in solid state between iron and barium carbonate, formation of barium hexaferrite
Total:	49.10			
Ba(CHCOO) <sub>2</sub> -Fe <sub>2</sub> O <sub>4</sub> (NaOH)	72–152	3.89	endo	two step water release
	152–200	3.31	endo	
	200–300	9.30	exo	decomposition of iron oxalate
	404–503	1.90	exo	decomposition of barium oxalate to barium carbonate
	545–662	1.23		reaction in solid state between iron oxide and barium carbonate, formation of barium hexaferrite
	662–722 <sup>b</sup>	0.41	exo	
722–861	1.79	exo		
Total:	21.83			
Ba(NO <sub>3</sub> ) <sub>2</sub> -FeC <sub>2</sub> O <sub>4</sub> (NaOH)	68–149	4.54	endo	two step water release
	149–211	4.58	endo	
	211–316	8.38	exo	decomposition of iron oxalate
	410–500	1.80	exo	decomposition of barium oxalate to barium carbonate
	533–631	1.02	exo	reaction in solid state between iron oxide and barium carbonate, formation of barium hexaferrite
	631–737 <sup>b</sup>	0.90		
737–888	1.74	exo		
Total:	22.96			

<sup>a</sup>  $T_i$  – initial temperature of thermal transformation,  $T_f$  – final temperature of thermal transformation.

<sup>b</sup> Continuous mass loss.

range. Table 1 summarizes the thermogravimetric obtained data for the investigated precursors (Fe/Ba ratio 12).

The nonisothermal analysis was associated with IR spectra and X-ray diffraction investigation for a complete and reliable assignment of thermal transformations. Hence, the following mechanism may be accepted:

– The first two decomposition reaction steps accompanied by endothermic effects represent

the release of humidity water and NH<sub>4</sub>OH, bonded lattice water.

– These reactions are followed by the oxidative decomposition of the iron oxalate present in the precursors and dehydration of  $\gamma$ -FeOOH to iron oxide. The phase analysis showed the existence of two phases: barium oxalate and iron oxide  $\gamma$ -Fe<sub>2</sub>O<sub>3</sub>. The XRD patterns recorded for the two types of precursors show a low crystallinity for the compounds obtained by precipitation with solution of BaOH, while

a high one is shown for the second type of precursors.

– The next thermal transformation which occurs practically in the same temperature range, respectively 400–500°C, consists in the decomposition of barium oxalate into barium carbonate. The phases discerned in the intermediates are BaCO<sub>3</sub> and iron oxides:  $\gamma$ -Fe<sub>2</sub>O<sub>3</sub> as main products and  $\alpha$ -Fe<sub>2</sub>O<sub>3</sub> in traces (4–7%). Although all the intermediates are crystalline, a better crystallinity is put into evidence for the precursors obtained by precipitation with NH<sub>4</sub>OH.

– The following thermal transformations are due to the transformation of  $\gamma$ -Fe<sub>2</sub>O<sub>3</sub> into  $\alpha$ -Fe<sub>2</sub>O<sub>3</sub> as well as to the reaction between iron oxides and BaCO<sub>3</sub> leading to mixed oxides. The thermogravimetric curves put into evidence for the two types of precursors reveal a different progress of these solid state reactions.

### 3.2.1. Precursors obtained by precipitation with NH<sub>4</sub>OH solution

The TG curve levels off in the 510–660°C (raw material Ba(HCOO)<sub>2</sub>) and 502–687°C (raw material Ba(NO<sub>3</sub>)<sub>2</sub>) ranges. The X-ray patterns of the intermediates obtained at 550°, 600°, and 650°C indicate the tendency of a gradual conversion of  $\gamma$ -Fe<sub>2</sub>O<sub>3</sub> into  $\alpha$ -Fe<sub>2</sub>O<sub>3</sub>. The transformation is complete at the temperature corresponding to the beginning of the mass loss. A single decomposition step is recorded in the 660–835°C (raw material Ba(HCOO)<sub>2</sub>) and 687–850°C (raw material Ba(NO<sub>3</sub>)<sub>2</sub>) ranges. In these temperature ranges,  $\alpha$ -Fe<sub>2</sub>O<sub>3</sub> reacts with BaCO<sub>3</sub> to form monoferrite BaFe<sub>2</sub>O<sub>4</sub>, which reacts further on with  $\alpha$ -Fe<sub>2</sub>O<sub>3</sub> to form hexaferrite. The first diffractions line corresponding to barium hexaferrite were detected at 750°C.

### 3.2.2. Precursors obtained by precipitation with NaOH solution.

The TG curves reveal two distinct reaction steps. In the first reaction step, which occurs in the 540–607°C (raw material Ba(CHCOO)<sub>2</sub>) and 533–631°C (raw material Ba(NO<sub>3</sub>)<sub>2</sub>) ranges, an amount of 36 and 28%, respectively, from BaCO<sub>3</sub> content is decomposed. The phase analysis put into evidence the formation of BaFe<sub>2</sub>O<sub>4</sub>. Simultaneously, weak lines corresponding to barium hexaferrite were also evi-

denced. One can advance two main reasons for the increased reactivity of the solid intermediates namely; the partially amorphous nature of the intermediates and a better mixing at molecular level of the cations, due to an advanced destruction of the initial raw materials structure.

This reaction is followed by a continuous mass loss, in the 607–722°C (raw material Ba(NO<sub>3</sub>)<sub>2</sub>) range.  $\gamma$ -Fe<sub>2</sub>O<sub>3</sub> is detected even at the beginning of the second well-defined decomposition step (~10%). The presence of this oxide at such a high temperature is due to the low degree of crystallinity of the samples. Similar conclusions were referred to by Macieas et al. [6].

Although the literature data [7–11] mentioned an exothermic effect associated with ferrite formation at ~750°C, it was not found in our case, due to the overlapping of the ferritization reaction with the decomposition of the precursors (e.g. decomposition of BaCO<sub>3</sub>).

At the final decomposition temperatures the residue contain three crystalline phases, respectively: barium hexaferrite (BaFe<sub>12</sub>O<sub>19</sub>), barium monoferrite (BaFe<sub>2</sub>O<sub>4</sub>), and iron oxide ( $\alpha$ -Fe<sub>2</sub>O<sub>3</sub>).

In order to obtain a pure barium hexaferrite the decomposition residues were submitted to further isothermal treatments for intervals of time ranging from 1 h to 30 h at 900°C. The phase analysis of the end products outlines the following reaction between BaFe<sub>2</sub>O<sub>4</sub> and  $\alpha$ -Fe<sub>2</sub>O<sub>3</sub>, when hexaferrite was obtained faster in the residues obtained from the precursors precipitated with NaOH solution. If, for this reaction, the amount of monoferrite is already consumed after 20 h annealing, for the other two, the diffraction lines characteristic for monoferrite are present even after 30 h of calcination at this temperature. Working with a molar ratio Fe/Ba=12, constant small amounts of  $\alpha$ -Fe<sub>2</sub>O<sub>3</sub> impurity phase (~9–11%) remained in the calcination residues even after an annealing time of 30 h.

In order to get a single phase sample the initial Fe/Ba ratio was slightly decreased. The pure hexaferrite was obtained at a value of the ratio which equals 10.5, in this condition the ferritization being complete after 20 h of calcination. The mean crystallite size of the obtained hexaferrite varies in the 420–470 Å range.

In Fig. 1 the IR spectra of the decomposition intermediates, obtained in the decomposition of the precursor on precipitation with NaOH solution (raw



Fig. 1. IR spectra of the precursor (precipitation with NaOH raw materials  $\text{FeC}_2\text{O}_4\text{-Ba}(\text{CHCOO})_2$ ) and its decomposition intermediate. (a) Initial precursor; (b) intermediate obtained at 200°C; (c) intermediate obtained at 300°C; (d) intermediate obtained at 400°C; (e) intermediate obtained at 500°C; (f) intermediate obtained at 700°C; and (g) intermediate obtained at 900°C (20 h calcination).

material  $\text{Ba}(\text{CH}_3\text{COO})_2$ , are given. The vibration assigned to the stretching modes of water and hydroxyl ions were put into evidence in the 2800–3400 and 676  $\text{cm}^{-1}$  ranges. These bands disappeared at temperature close to 200°C due to the loss of water molecules. The presence of the oxalate anion was put into evidence through the band present in the 1657–740  $\text{cm}^{-1}$  range. The pattern successively changed above 200°C until 500°C indicating its total decomposition. In the temperature range of 500–850°C, carbonate intermediates were isolated, which exhibit a very strong band at  $\sim 1430 \text{ cm}^{-1}$  characteristic of the presence of  $\text{CO}_3^{2-}$  anion. The band disappeared at the completion of the reaction (900°C). After the decomposition of iron oxalate, strong absorption bands, due to the iron–oxygen bonds, (corresponding to iron located in octahedral and tetrahedral position respectively), were observed in the 540–540  $\text{cm}^{-1}$  range. The slight shift of the bands position connected with the changes in their intensities ratio are due to the transformation of iron oxides into hexaferrite during heating.

The measured value of the saturation magnetization for the obtained barium hexaferrite was 47.58 emu/g lower than the literature value of 71 emu/g [12]. A study concerning the optimization of the magnetic properties will be carried out later.

#### 4. Conclusions

1. New precursors of barium hexaferrite synthesized by an original method have been chemically and physico-chemically characterized.
2. The relation between precursors' history, thermal behavior and phase composition of the decomposition intermediates was investigated
3. Although the decomposition behavior was mostly the same for the two types of precursors, differences were observed in the solid state formation reaction of barium hexaferrite.
4. The proper ratio for the composition  $\text{BaO}.n\text{Fe}_2\text{O}$  ( $n=5.25$ ) was found in order to get single phase barium hexaferrite with a mean crystallite size in the 420–470 Å range.

#### Acknowledgements

The authors gratefully acknowledge the financial support of the Department of Education under GRANT No. 5009

#### References

- [1] O. Kubo, T. Ido, H. Jokoyama, IEEE Trans. Magn, MAG-18, 1982, p. 1122.
- [2] M.T. Shrik, W.R. Buessen, J. Am. Ceram. Soc. 53 (1970) 192.
- [3] T. Fujiwara, IEEE Trans. Mang. 21 (1985) 1480.
- [4] O. Carp, E. Segal, M. Brezeanu, R. Barjega, N. Stanica, J. Thermal Anal. 50 (1997).
- [5] H. Klug, L. Alexander (Eds.), X-ray Diffraction Procedure, John Wiley and Sons, New York, 1962, p. 461.
- [6] M. Marcias, J. Morales, J.L. Tirado, C. Valera, Thermochim. Acta 133 (1988) 107.
- [7] W. Ross, J. Am. Ceram. Soc. 63 (11–12) (1980) 601.
- [8] A. Srivastava, P. Singh, V.G. Gunjekar, A.P.B. Sinha, Thermochim. Acta 86 (1985) 77.
- [9] K. Higuchi, S. Naka, S. Hirano, Adv. ceram. Mater. 1(1) (1986) 121.
- [10] E. Luchini, S. Mariani, F. Delben, S. Paoletti, J. Mater. Sci. 19 (1984) 121.
- [11] S.D. Kulkarni, C.E. Desphande, J.J. Shrotri, V.G. Gunjekar, S.K. Date, Thermochim. Acta 153 (1989) 47.
- [12] S. Hiraga, K. Okotani, Ferrite, Maruzen, 1986, p. 129.